Continuous Nucleocytoplasmic Shuttling Underlies Transcriptional Activation of PPARγ by FABP4 †

ARTICLE *in* BIOCHEMISTRY · JULY 2007

Impact Factor: 3.02 · DOI: 10.1021/bi700047a · Source: PubMed

4 AUTHORS, INCLUDING:

Stephen Ayers
Personalis Inc.
22 PUBLICATIONS **389** CITATIONS
SEE PROFILE

Noa Noy
Case Western Reserve University
120 PUBLICATIONS **5,865** CITATIONS
SEE PROFILE

Continuous Nucleocytoplasmic Shuttling Underlies Transcriptional Activation of PPARγ by FABP4[†]

Stephen D. Ayers,[‡] Katherine L. Nedrow,[§] Richard E. Gillilan,[||] and Noa Noy*[,‡,§]

Division of Nutritional Sciences, Cornell University, Ithaca, New York 14853, Department of Pharmacology, Case Western Reserve School of Medicine, Cleveland, Ohio 44106, and Macromolecular Diffraction Facility of the Cornell High-Energy Synchrotron Source, Cornell University, Ithaca, New York 14853

Received January 10, 2007; Revised Manuscript Received April 4, 2007

ABSTRACT: FABP4 delivers specific ligands from the cytosol to the nuclear receptor PPARγ in the nucleus, thereby facilitating the ligation and enhancing the transcriptional activity of the receptor. Here, we delineate the structural features that underlie the nucleocytoplasmic transport of FABP4. The primary sequence of FABP4 does not harbor a readily identifiable nuclear localization signal (NLS). However, such a signal could be found in the three-dimensional structure of the protein and was mapped to three basic residues that form a functional NLS stabilized by the FABP4/PPARγ ligand troglitazone. We show that FABP4 is also subject to active nuclear export. Similarly to the NLS, the nuclear export signal (NES) is not apparent in the primary sequence, but assembles in the tertiary structure from three nonadjacent leucine residues to form a motif reminiscent of established NES. The data demonstrate that both nuclear export and nuclear import are critical for enabling FABP4 to enhance the transcriptional activity of PPARγ. Additionally, the observations provide insight into the fundamental question of how proteins are activated by ligands. Such an activation may be understood by the "induced-fit" model, which states that ligand-induced conformational changes precede activation of a protein. Alternatively, the "pre-existing equilibrium" hypothesis postulates that activated conformations exist within the repertoire of apoproteins, and that ligands do not induce these but merely stabilize them. Studies of the subcellular localization of FABP4 support the validity of the "pre-existing equilibrium" model for the ligand-controlled activation of the nuclear import of FABP4.

Small lipophilic compounds, such as retinoic acid and long chain fatty acids and some of their metabolites, can regulate gene expression by activating specific members of the superfamily of nuclear hormone receptors. Retinoic acid activates retinoic acid receptors (RARα, β, γ). The transcriptional activities of long chain fatty acids and their active derivatives are mediated by several classes of nuclear receptors, the best characterized of which are the peroxisome proliferator-activated receptors (PPARα, δ, γ (*1*)). Among PPARs, PPARγ is of special interest. This receptor is involved in regulation of adipocyte differentiation (*2*, *3*), modulation of insulin sensitivity (*4*, *5*), and macrophage function (*6*, *7*). Activation of PPARγ also inhibits proliferation and induces apoptosis in various types of carcinomas (*8*). Like other PPARs, PPARγ displays a broad ligand selectivity and binds various unsaturated long chain fatty acids as well as some eicosanoids (*9*). Thiazolidinediones, synthetic PPARγ-selective ligands, are in current use in treatment of metabolic disorders such as type 2 diabetes and arteriosclerosis (*10*, *11*), and may be efficacious in treatment of various cancers (*12*, *13*).

In addition to nuclear receptors, many lipophilic compounds in cells associate with intracellular lipid-binding proteins (iLBP), a family of small (~15 kDa) proteins that includes cellular retinol-binding proteins, cellular retinoic acid-binding proteins (CRABP-I, II), and nine known isotypes of fatty acid binding proteins (FABP (*14*)). The iLBPs share a remarkably similar β-clam structure composed of two 5-stranded orthogonal β-sheets that form a ligand binding pocket capped by a helix−loop−helix "lid" (*15*−*17*). CRABPs display strict selectivities toward retinoic acid (*18*−*21*). In contrast, FABPs associate with a broad array of hydrophobic ligands, reminiscent of that of PPARs (*22*−*24*).

The shared ligand selectivities of some iLBPs and some nuclear receptors suggest that specific members of the two classes of proteins may cooperate in regulating the biological activities of their common ligands. Such a cooperation is also suggested by overlapping tissue expression profiles and by involvement in similar biological functions. For example, PPARγ and FABP4 (A-FABP, aP2) are coexpressed in adipocytes and in macrophages, and, like PPARγ, FABP4 is involved in adipocyte differentiation, glucose homeostasis, and inflammation (*25*−*30*). Also similarly to PPARγ, expression of FABP4 is associated with antiproliferative

[†] This work was supported by NIH Grant RO1 DK60684 to N.N. S.D.A. was supported by NIH Grant T32-DK715827.

* Address correspondence to this author at Department of Pharmacology, Case Western Reserve University, Biomedical Research Building, Rm 724, 10900 Euclid Avenue, Cleveland, OH 44106-4965. Phone: 216-368-0302. E. mail: noa.noy@case.edu.

[‡] Division of Nutritional Sciences, Cornell University.

[§] Case Western Reserve School of Medicine.

[||] Macromolecular Diffraction Facility of the Cornell High-Energy Synchrotron Source, Cornell University.

10.1021/bi700047a CCC: $37.00
Published on Web 05/22/2007

activities in several types of carcinomas (*31*, *32*). Indeed, our recent studies demonstrated that three iLBPs, namely, CRABP-II, FABP4, and FABP5 (K-FABP, eFABP, mal1), selectively cooperate with the nuclear receptors RAR, PPARγ, and PPARδ, respectively (*21*, *33*−*36*). These studies established that, upon association with particular ligands, these binding proteins translocate from the cytosol to the nucleus, that they engage in direct protein−protein interactions with their "cognate" receptors, and that the resulting complex mediates "ligand-channeling" from the binding protein to the receptor. Consequently, the binding proteins significantly enhance the transcriptional activities of the respective receptors.

Although FABP4 and FABP5 bind multiple ligands, only particular compounds trigger their nuclear transport (*34*). FABP5 translocates into the nucleus in response to ligands that activate PPARδ but not upon treatment with PPARγ ligands. Conversely, in accordance with its functional cooperation with PPARγ, FABP4 mobilizes to the nucleus only in response to ligands that activate this receptor. These observations raise the question of the structural features that underlie the induction of nuclear import of FABPs by particular "activating" ligands. Several models currently exist to explain the activation of proteins by ligands. These include the classical "lock and key" model, which highlights shape complementarity between a protein and a ligand, and the "induced fit" model, which suggests that ligand-binding induces a protein to undergo conformational changes, and that ligand-triggered structural rearrangements precede the formation of the activated state (*37*). In contrast, the more recent "pre-existing equilibrium/conformational selection" model proposes that the native state of a protein is not defined by a single conformation, but rather, that proteins in solution occupy an ensemble of states, including conformations that are compatible with ligand-binding (*38*). According to this theory, the holo-conformation is adopted not as a result of ligand-binding, but by virtue of being stabilized by it. Evidence for pre-existing equilibria as a mechanism for protein interactions *in vitro* has been reported (*39*, *40*), but the relevance of the model for the biological activities of proteins remains unclear.

The iLBPs do not harbor a recognizable nuclear localization signal (NLS) in their primary sequences. However, a recent study of one member of this family, CRABP-II, demonstrated that such a signal can be identified in the protein's 3-dimensional fold. A comparison between the structures of holo- and apo-CRABP-II revealed that, upon ligand-binding, three basic residues, located at the helix−loop−helix region of the protein, shift their orientation to place their side chains in close alignment with a "classical" NLS. It was further established that these residues, K20, R29, K30, indeed comprise the ligand-triggered NLS of the protein (*33*). The structural homology between CRABP-II and FABPs suggest that their nuclear import may be mediated by similar NLS. The present study was thus undertaken in order to gain insight into the structural features that underlie the activation of nuclear import of FABP4 by specific ligands, and to assess the importance of nucleocytoplasmic trafficking of the protein for its ability to enhance the transcriptional activity of its cognate receptor, PPARγ.

EXPERIMENTAL PROCEDURES

Reagents. ANS and troglitazone were purchased from Molecular Probes (Eugene, OR) and from Cayman Chemical (Ann Arbor, MI), respectively. Leptomycin B was purchased from Sigma-Aldrich, St. Louis, MO.

Constructs. The coding sequence mFABP4 in pBluescript (provided by David Bernlohr) was subcloned into pSG-5 and pEGFP-C2. Mutant forms of FABP4 were generated by overlap extension PCR as described (*41*). A bacterial expression vector of histidine-tagged FABP4 was constructed by subcloning its coding sequence from pBluescript into pET28a+.

Proteins. Histidine-tagged proteins were expressed in the *Escherichia coli* strain BL21. Protein expression was induced overnight at 25 °C with 0.5 mM isopropyl-β-D-thiogalactopyranoside (IPTG). Bacteria were pelleted and lysed in lysis buffer (20 mM Tris pH 8.0, 0.5 mM NaCl, 100 μM phenylmethylsulfonyl fluoride (PMSF)) supplemented with lysozyme (in 1 mM Tris, pH 7.5, 5 mM $MgCl_2$ and 0.13 mM $CaCl_2$) and DNAse I (30 min 37 °C). Protein was purified using his-trap column (Amersham, Piscataway, NJ) washed with lysis buffer, eluted with 0.5 M imidazole, and dialyzed against lysis buffer.

Cells. COS-7, MCF-7, and NIH 3T3 cells were purchased from the American Type Culture Collection (Manassas, VA). COS-7 and MCF-7 cells were cultured in Dulbecco's modified Eagle's medium (DMEM, Mediatech Inc., Herdnon, VA) supplemented with 10% fetal bovine serum (FBS, Atlanta Biologicals, Lawrenceville, GA) and were transfected using Fugene (Roche, Indianapolis, IN) according to the protocol of the manufacturer. NIH3T3 cells were cultured in 10% calf serum (CS, Atlanta Biologicals, Lawrenceville, GA) and transfected with Superfect (Qiagen) according to the protocol of the manufacturer.

Fluorescence titrations were carried out using a Fluorolog 2 DMIB spectrofluorometer (SPEX Instruments, Edison, NJ). Protein **(**1 μM in 10 mM HEPES, pH 8.0, 400 mM KCl, 0.1 mM EDTA, 0.5 mM DTT) was titrated with ANS (in methanol) by sequential additions of ANS in 0.1 μM increments. Progress of titrations was followed by monitoring the fluorescence of ANS (λ_{ex} = 375 nm, λ_{em} = 475 nm). Titration curves were analyzed by fitting to a binding equation (*42*) to yield the number of binding sites and K_d. Analyses were carried out by using Origin 6.0 software (MicroCal Software Inc., Northampton, MA).

Fluorescence Competition Titrations. FABP4 (0.5 μM) was complexed with ANS at a molar ratio of 1:0.8. The FABP4 ligand troglitazone was added at increasing concentrations (0.1−1 μM) and mixtures allowed to equilibrate for 1 h at room temperature. Displacement of ANS from FABP4 was monitored by following the decrease in ANS fluorescence. K_d for the nonfluorescent ligand was derived from the EC_{50} of the competition curve and the previously determined K_d for ANS.

Confocal Fluorescence Microscopy. COS-7 cells were seeded on 35 mm plates in DMEM supplemented with 10% charcoal treated fetal bovine serum and transfected with vectors encoding GFP-tagged FABP4 or mutant counterparts (300 ng). Four hours after transfection, the medium was changed to serum-free DMEM and cells were incubated overnight. Under these conditions, the expression levels of

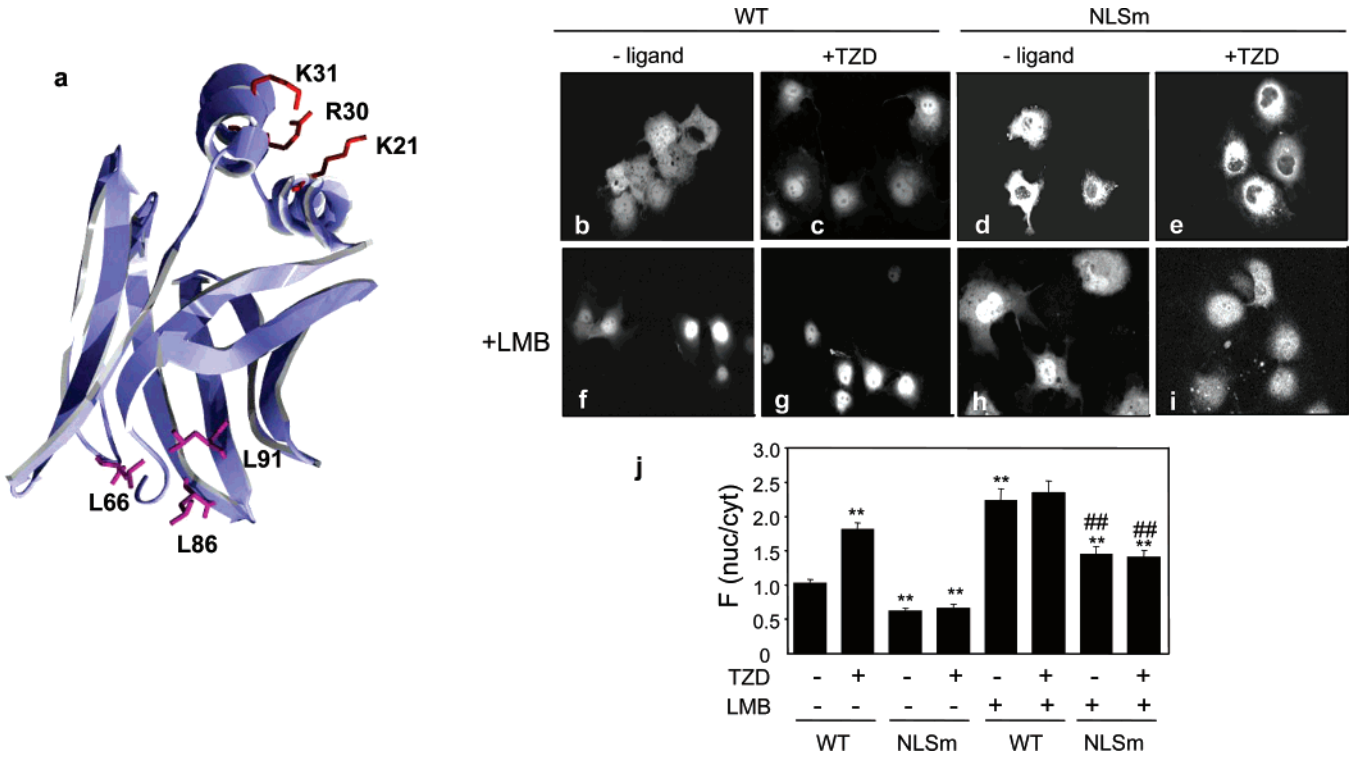

FIGURE 1: Nuclear import of FABP4 is mediated by residues K21, R30, and K31. (a) X-ray crystal structure of FABP4 (ref *47*, PDB entry 1LIB). Highlighted are residues that comprise the putative NLS (K21, K30, and K31, red), and the putative NES (L66, L86, L91, purple) of the protein. The structure was generated in DeepView (http://ca.expasy.org/spdbv/) and rendered in Povray (http://www.povray.org/). (b−j) COS-7 cells were transfected with expression constructs for WT-GFP-FABP4 (b,c,f,g) or GFP-FABP4-K21A/R30A/K31A (NLSm) (d,e,h,i). Cells were treated with vehicle, or troglitazone (TZD, 1 μM) for 1 h in the absence or presence of the nuclear export inhibitor LMB (5 ng/mL), and imaged. (j) The ratio of fluorescence in the nucleus and the cytosol in 25−50 cells under each condition was quantitated. Data (mean ± SEM) were analyzed with 1-tailed Student's *t* tests with pooled variances. (**) $P < 0.05$ compared to untreated WT-FABP4; (##) $P < 0.05$ compared to WT FABP4+LMB.

all tested tagged proteins were similar as verified by visualization and by semiquantitative PCR analyses. Cells were treated with troglitazone (1 μM) for 1 h prior to imaging. Cells were visualized using a Leica confocal microscope (Leica, Bannockburn, IL), using a 40× dipping lens and argon 488 nm laser. Images were analyzed using ImageJ 1.33u (Wayne Rasband, National Institutes of Health, U.S.A.). The subcellular localization of a GFP-tagged protein was expressed as the ratio of image density of a representative area of the nucleus over the image density of a representative area of cytoplasm.

Knockdown Experiments. FABP4 siRNA (Silencer predesigned 9956) and control siRNA (Silencer negative control #1) were purchased from Ambion (Austin, TX). Cells (1.5×10^5) were transfected with using Superfect (Qiagen) using the manufacturer's protocol.

Transactivation Assays. COS-7 cells were cultured in 6-well plates in DMEM supplemented with 10% charcoal-treated FBS, and transfected with a $(PPRE)_3$-luciferase reporter vector (300 ng), and expression vectors for PPARγ (in pCDNA, 200 ng), and FABP4 or corresponding mutants (in pEGFP-C2, 400 ng). Transfection efficiency was monitored by cotransfection of pCH110, encoding β-galactosidase (200 ng). Cells were grown for 24 h, the medium was replaced by DMEM, cells were treated with troglitazone for 24 h and lysed, and luciferase activity was measured by the Luciferase Assay System (Promega, Madison, WI) and normalized to β-galactosidase activity. When mentioned, siRNA was transfected simultaneously with DNA using the DNA transfection protocol.

Semiquantitative PCR. Total RNA was extracted using RNeasy (Qiagen) and cDNA synthesized using GeneAmp RNA PCR Core Kit (Applied Biosystems). PCR amplification was conducted using 2 min at 94 °C, 23 or 18 cycles of 15 s at 94 °C, and 30 s at 65 °C. Amplification was carried out using the following primer sets:

cJun, forward: 5′-TGCAAAGATGGAAACGACCTT-3′
reverse: 5′-CAGGTTCAGGGTCATGCTCTG-3′
mmFABP4, forward: ACTGGGCCAGGAATTTGACG
reverse: CATGTACCAGGACACCCCCATC
β-actin, forward: 5′-GTGGGCCGCTCTACGCACCAA-3′
reverse: 5′-GGGTCATCTTTTCACCGGTTG-3′

Quantitative Real Time PCR (Q-PCR). Total RNA was extracted using the RNeasy kit (Qiagen), and cDNA generated using GeneAmp RNA PCR (Applied Biosystems). Q-PCR was performed in quadruplicates using TaqMan chemistry and Assays on Demand probes (Applied Biosystems) for cJun (Hs00277190_s1) and FABP4 (Hs00609791_m1). 18S ribosomal RNA (4319413E-0312010) was used as a loading control. Analysis was carried out using the relative standard method (Applied Biosystems Technical Bulletin No. 2).

RESULTS

Nuclear Import of FABP4 Is Mediated by K21, R30, and R31. The NLS of CRABP-II consists of three basic residues

located in the helix−loop−helix region of the protein (*33*). The structural homology of CRABP-II and FABP4 raises the possibility that nuclear import of the latter protein may be mediated by a similar NLS, composed of the corresponding residues, K21, R30, and K31 (Figure 1a). To explore this possibility, an FABP4 mutant in which these residues were replaced by alanines (FABP4-K21A/R30A/K31A, NLSm) was generated. To examine whether the mutations altered the overall fold of the protein, the equilibrium dissociation constants (K_d) for binding of the synthetic FABP4/PPARγ ligand troglitazone to WT-FABP4 and the mutant lacking the putative NLS were measured. Proteins were overexpressed in *E. coli* and purified. K_ds of FABP4 and its mutants for troglitazone were measured by competition fluorescence titrations (*34*, *43*). In these, the fluorescent fatty acid anilinonaphthalene-8-sulfonic acid (ANS) was used as a probe. FABP4 was precomplexed with ANS and the complex titrated with troglitazone. The displacement of the probe from the protein was monitored by following the decrease in its fluorescence, and competition curves were analyzed to obtain the respective K_d. K_ds for association of WT-FABP4 and of FABP4-K21A/R30A/K31 with ANS were found to be 32 ± 4 (n = 4) and 26 ± 8 nM (n = 3), respectively. Troglitazone associated with the two proteins with K_ds of 17 ± 3 (n = 4) and 60 ± 6 nM (n = 5). The ligand-binding affinity of the mutant is thus similar to that of the WT protein, indicating that the mutations did not significantly alter the folding of the protein or hamper its tight association with ligands.

The subcellular localizations of FABP4 and its K21A/R30A/K31A mutant were then studied. Mammalian expression vectors encoding FABP4 or the mutant fused with green fluorescent protein (GFP) were used. The constructs were transfected into COS-7 cells, and the localization of the proteins was examined by confocal fluorescence microscopy. As a control, cells were transfected with a plasmid expressing GFP alone. GFP was distributed across the cells (data not shown and ref *33*), most likely reflecting that its high expression level resulted in leakage into the nucleus even in the absence of a specific NLS. To examine the subcellular location of GFP-FABP4 and its NLS mutant, cells were maintained in delipidated medium, treated with vehicle or troglitazone for 1 h, and imaged (Figure 1b−e). To obtain statistically meaningful data, the ratio of fluorescence intensity in the nuclei and cytosol of 30−50 cells under each condition was quantitated (Figure 1j). In the absence of ligand, GFP-FABP4 partitioned between the cytosol and the nucleus, and, as previously reported (*34*), addition of troglitazone markedly increased the fraction of the protein in the nucleus. In contrast, the K21A/R30A/K31A mutant was largely excluded from the nucleus both in the absence and in the presence of the ligand (Figure 1d,e). Hence, residues K21, R30, and K31 are critical for nuclear import of FABP4. The striking nuclear exclusion of the FABP4-NLSm is notably different than that observed for CRABP-II lacking its NLS. Specifically, the CRABP-II-NLSm is unable to undergo ligand-induced nuclear import, but is not excluded from the nucleus and displays a diffuse distribution across the cell (*33*). The nuclear exclusion of FABP4-NLSm thus suggests that, in addition to its nuclear import, FABP4 may also be actively exported from the nucleus, and that this process dominates in the absence of a functional NLS.

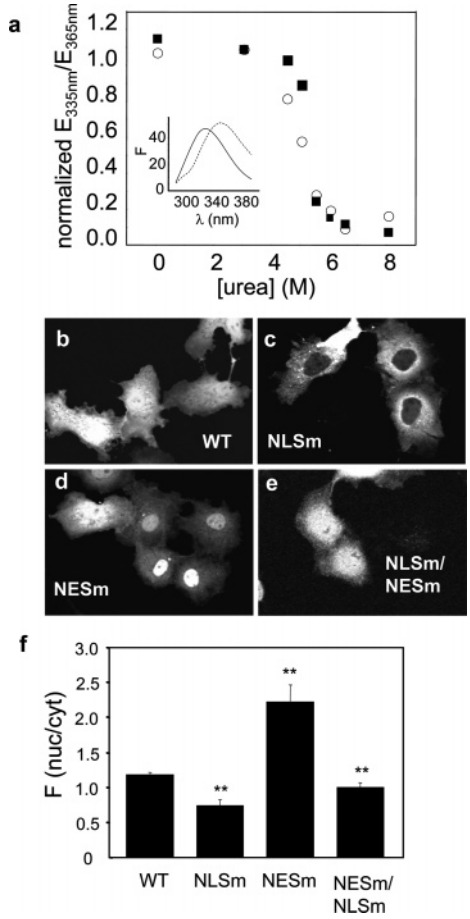

FIGURE 2: Nuclear export of FABP4 is mediated by residues L66, L86, and L91. (a) The fluorescence emission spectra of FABP4 (1 μM, λex 280 nm) in the absence (solid line) or presence of 8 M urea (dashed line) are shown in the inset. Urea-induced unfolding of WT-FABP4 (squares) and FABP4-NESm (circles) was followed by monitoring the emission shift, presented as the ratio of fluorescence at 335 and 365 nm. Normalized values are shown. (b−e) COS-7 cells were transfected with expression constructs for WT-GFP-FABP4 (b), or GFP-FABP4-NLSm (c), or GFP-FABP4-NESm (d), or GFP-FABP4 containing mutations in both the putative NLS and NES (NLSm/NESm) (e). (f) The ratio of fluorescence in the nucleus and the cytosol in 20−40 cells under each condition was quantitated, and data (mean ± SEM) were analyzed with 1-tailed Student's t tests. (**) $P < 0.05$.

FABP4 Is Exported from the Nucleus by the CRM1-Dependent Export Machinery. To explore the possibility that FABP4 is actively exported from the nucleus, the subcellular localization of the protein was examined in the presence of leptomycin B (LMB), a compound that specifically inhibits nuclear export mediated by the CRM1 export system (*44*, *45*). In the presence of LMB, GFP-FABP4 was predominantly nuclear, and its nuclear localization was slightly enhanced upon addition of troglitazone (Figure 1f,g). In contrast with the nuclear exclusion of the NLSm in the absence of LMB, the mutant partitioned between the cytosol and the nucleus in the presence of the nuclear export inhibitor. Hence, abolishing nuclear import by mutating the NLS, and inhibiting active nuclear export using LMB, resulted in a protein which, similarly to GFP alone, passively distributed across the cell. Taken together, the data in Figure 1 demonstrate that the FABP4 is exported from the nucleus by the CRM1 export system, and that the protein's nuclear import critically requires residues K21, R30, and K31 and

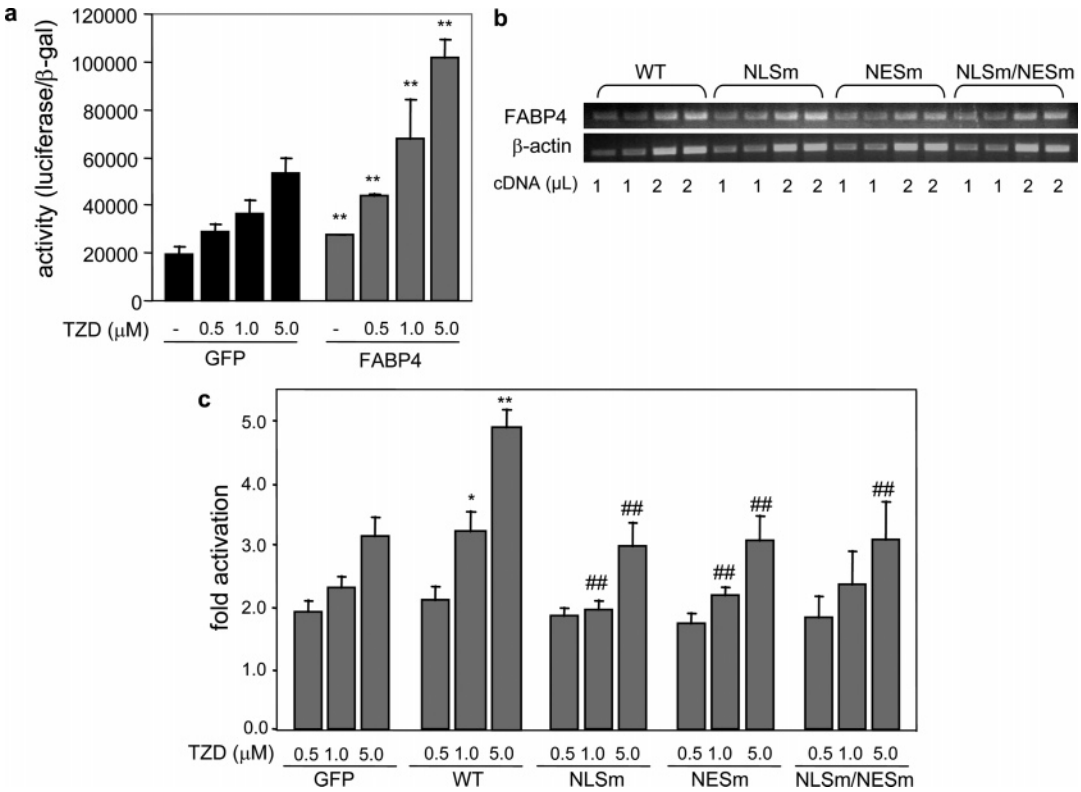

FIGURE 3: Nuclear import and export are required for FABP4-mediated enhancement of the transcriptional activity of PPARγ. (a) COS-7 cells were cotransfected with a $(PPRE)_3$-luciferase reporter vector, an expression vector for PPARγ (in pCDNA), and a vector harboring GFP or GFP-tagged FABP4 (in pEGFP-C2). Transfection efficiency was monitored by cotransfection of pCH110, encoding β-galactosidase. Cells were treated with troglitazone or vehicle overnight prior to lysis and measurements of luciferase activity. Luciferase activity was normalized to β-gal activity. Data (mean $\pm$ SEM, $n = 3$) of a representative experiment are shown. Similar results were obtained in three independent experiments. (b) COS-7 cells were transfected with expression plasmids for GFP-FABP4, and its mutants and levels of mRNA were determined by semiquantitative PCR. β-Actin was used as a loading control. (c) Transactivation assays were carried out in COS-7 cells transfected with the denoted FABP4 constructs as described in the legend to panel a. Fold activation relative to the activity in the absence of ligand is shown. Data (mean $\pm$ SEM) were analyzed with a 1-tailed Student's t test. (*) $P < 0.1$, (**) $P < 0.05$ compared to the corresponding GFP controls. ($^{\#}$) $P < 0.1$, ($^{\#\#}$) $P < 0.05$ compared to WT-FABP4. In both panel a and panel c, $n = 3$.

dominates in the presence of an activating ligand such as troglitazone.

Identification of the Nuclear Export Signal of FABP4. Nuclear export by the CRM1-dependent nucleocytoplasmic shuttling proteins is mediated by a nuclear export signal (NES) composed of one or more leucine-rich motifs with the consensus motif L-X_2-3-L-X_2-3-L-X-L (*46*). However, no such motif can be identified in the primary sequence of FABP4. We thus considered the possibility that, similarly to the NLS which is not found in the primary sequence but can be identified in the folded FABP4, an NES may be found in the tertiary structure of the protein. Inspection of the 3-dimensional X-ray crystal structure of FABP4 (*47*) in search for a leucine-rich region at the surface of the protein revealed three leucine residues, L66, L86, and L91, whose side chains protrude from the protein at the bottom of the ligand binding pocket (Figure 1a). Though nonadjacent in the primary sequence, these residues form a compact leucine-rich motif in the tertiary structure.

An FABP4 mutant in which these leucines were exchanged for alanines (FABP4-L66A/L86A/L91A, NESm) and a construct containing mutations in both the NLS and the putative NES (NLSm/NESm) were then generated. The mutants were bacterially expressed, and the K_ds that characterize their interactions with ANS and with troglitazone were measured by fluorescence competition titrations. The ligand binding affinities of both mutants were essentially indistinguishable from those of the wild-type protein, indicating that they are structurally intact (not shown). To further examine whether the NES mutation may perturb the overall folding of the protein, the sensitivity of the NESm to urea-induced denaturation was examined. As shown in Figure 2a (inset), urea-induced unfolding of FABP4 is associated with a shift in the protein's fluorescence emission spectrum. The progressive unfolding of the protein could thus be followed by monitoring the shift in fluorescence emission maxima. The data (Figure 2a) demonstrate that the behavior of the mutant upon exposure to urea was very similar to that of the WT protein, supporting the conclusion that the mutations did not affect the global folding of FABP4.

Expression vectors harboring cDNAs for the mutant proteins fused with GFP were generated and transfected into COS-7 cells, and proteins were imaged by confocal fluorescence microscopy. WT-FABP4 distributed across the cell (Figure 2a,e), and FABP4-NLSm was excluded from the nucleus (Figure 2b,e). In contrast, FABP4 harboring mutations in the putative NES displayed a degree of nuclear localization similar to that observed upon treatment with the nuclear export inhibitor LMB, i.e., was localized predominantly in the nucleus (Figure 2c,e). Mutation of both the NLS and NES residues resulted in a protein that, similarly to GFP alone, distributed across the cell (Figure 2d,e). Hence, L66, L86, and L91 are critical for nuclear export of FABP4. These observations also demonstrate that, in the

absence of its NES, FABP4 mobilizes to the nucleus even in the absence of ligand, suggesting that the population of the apoprotein contains an import-competent conformation (see Discussion).

Enhancement of the Transcriptional Activity of PPARγ by FABP4 Requires Both the NLS and the NES. The functional importance of nuclear/cytoplasmic shuttling of FABP4 was investigated by transcriptional activation assays. Assays were conducted in COS-7 cells, which express low levels of FABP4 (data not shown). Cells were cotransfected with a luciferase reporter construct driven by a PPAR response element (PPRE), together with an expression construct for FABP4. Cells were treated with troglitazone, and reporter expression was measured (Figure 3a). In accordance with its reported function in direct delivery of ligands to PPARγ (*34*), ectopic expression of FABP4 enhanced the ligand-induced, PPARγ-mediated activation of the reporter. To examine the importance of the NLS and the NES residues for the enhancement of PPARγ activity by FABP4, cells were transfected with constructs harboring cDNA for GFP-tagged WT-FABP4 or corresponding mutants. All constructs displayed similar levels of expression of mRNA (Figure 3b) and protein, as estimated by GFP fluorescence. Transactivation assays were then carried out (Figure 3c). The data showed that mutation of either the NLS or the NES of FABP4 completely abolished the ability of the protein to enhance PPARγ activity.

To further investigate the involvement of FABP4 in activation of PPARγ, transactivation assays were carried out in NIH3T3 cells. These cells endogenously express a high level of FABP4, allowing for examining whether decreasing the expression of the binding protein affects receptor activity. Cells were transfected with FABP4 siRNA, resulting in an 80−90% decrease in FABP4 expression (Figure 4a). The decrease markedly inhibited troglitazone-induced activation of a PPARE-driven reporter (Figure 4b), further demonstrating that FABP4 is necessary for efficient ligand-induced activation of PPARγ. The effects of introducing mutants that lack either the NLS or NES signatures were then examined (Figure 4c). Strikingly, ectopic overexpression of either mutant dramatically inhibited the activity of PPARγ.

The ability of FABP4 to enhance the transcriptional activity of PPARγ, and the requirement for nuclear/cytosolic trafficking for such an activity, was then examined in the context of an endogenous target gene. It was previously reported that, in colon cancer cells, troglitazone upregulates the expression of cJun (*48*). We thus examined whether this gene may be a direct target of PPARγ in MCF-7 mammary carcinoma cells, which were reported to express low levels of FABP4 (*2*, *49*, *50*). In agreement with the behavior observed in colon cancer cells, the expression level of cJun mRNA in MCF-7 cells increased upon a 30 min treatment with troglitazone, and was elevated further following a 2 h incubation (Figure 5a). The rapid response of *cJun* expression to activation of PPARγ suggests that this gene may comprise a direct target for transcriptional regulation by the receptor. To examine this possibility, the effect of the protein synthesis inhibitor cycloheximide on the induction was studied. Cycloheximide treatment will abolish secondary events that require *de novo* protein synthesis, but will not affect direct transcriptional responses. The analysis (Figure 5b) showed that cJun mRNA was similarly upregulated by troglitazone

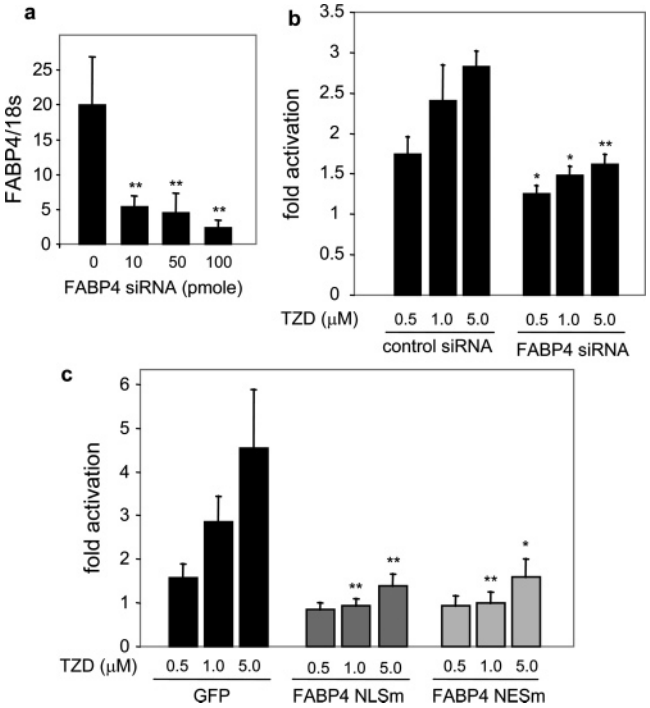

FIGURE 4: FABP4 is critical for efficient activation of PPARγ in NIH3T3 cells. (a) NIH3T3 cells were transfected with 10, 50, or 100 pmol of FABP4-siRNA for 24 h, and expression of FABP4 mRNA was assessed using Q-PCR. (b) Transactivation assays in NIH3T3 cells transfected with FABP4 siRNA (10 pmol). (c) Transactivation assays in NIH3T3 cells transfected with the denoted FABP4 constructs (in pEGFP-C2). Assays were carried out as described in the legend to Figure 3. Data were analyzed with a 1-tailed Student's *t* test with pooled variances. In panel a (*) $P < 0.1$, (**) $P < 0.05$, in panel b (**) $P < 0.05$ compared to control siRNA. In panel c * and ** indicate $P < 0.1$ and $P < 0.05$, respectively, compared to the GFP control. In all panels, $n = 3$.

in the absence and in the presence of cycloheximide, demonstrating that *cJun* is indeed a direct target for PPARγ signaling. The effect of FABP4 and its NLS and NES mutants on PPARγ-mediated upregulation of cJun expression was then investigated. MCF-7 cells were transfected with an expression construct for WT-FABP4, or the corresponding mutants, and treated with troglitazone for 2 h, and cJun mRNA levels were assessed by Q-PCR (Figure 6). Ectopic expression of FABP4 significantly enhanced troglitazone-induced upregulation of cJun, while expression of FABP4 carrying mutations in either the NLS or the NES had little effect. The data thus indicate that both its nuclear import and its nuclear export are required for enabling FABP4 to enhance transactivation by PPARγ.

DISCUSSION

Many proteins that do not contain recognizable nuclear import or export signals in their primary sequence can nevertheless move between the cytoplasm and the nucleus, raising the question of how their trafficking is accomplished (*51*−*54*). We show here that, although FABP4 does not harbor readily identifiable localization signals, it undergoes a ligand-induced nuclear import as well as a ligand-independent active nuclear export. The data demonstrate that, as in the case of the homologue CRABP-II (*33*), nuclear import of FABP4 is mediated by three basic residues, K21, R30, and K31. This functional NLS, which is stabilized by

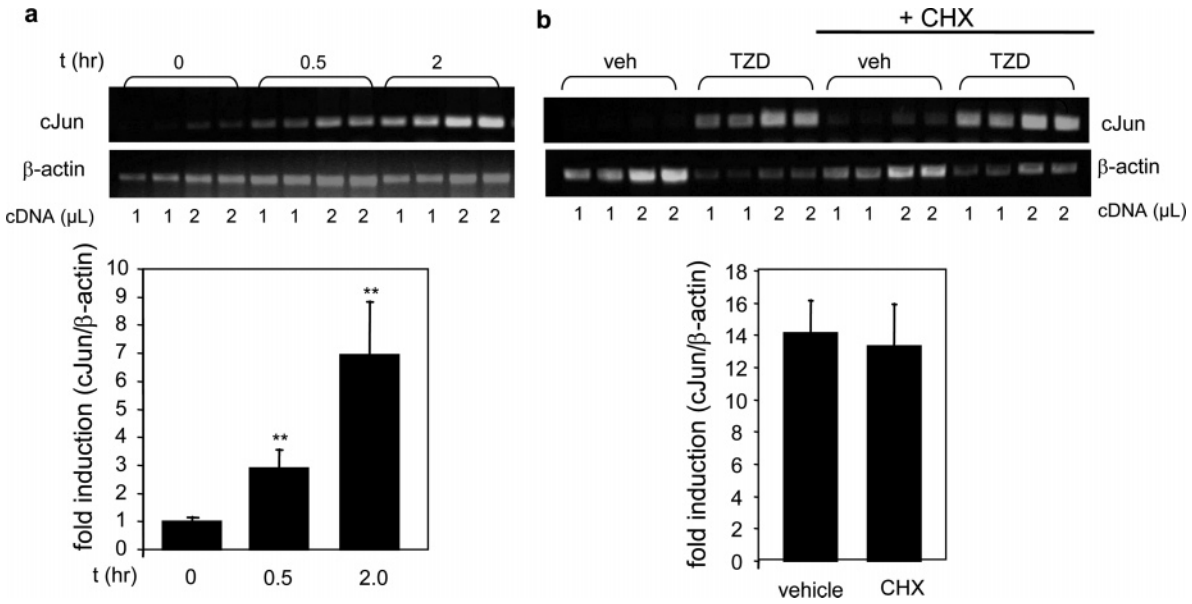

FIGURE 5: *cJun* is a direct target gene for PPARγ in MCF-7 cells. (a) MCF-7 cells were treated with vehicle or troglitazone (10 μM) for the denoted periods of time. Level of cJun mRNA was measured by semiquantitative PCR. Lower panel: quantitation of band intensities normalized to the β-actin loading control. Data were analyzed with a 1-tailed Student's *t* test with pooled variances. At 0.5 h $P < 0.025$, at 2.0 h $P < 0.005$ compared to untreated cells. $N = 4$. (b) MCF-7 cells were pretreated with vehicle or cycloheximide (CHX) for 15 min prior to treatment with vehicle or with troglitazone (10 μM, 1 h). Expression levels of cJun mRNA was measured by semiquantitative PCR. Lower panel: quantitation of band intensities normalized to the β-actin loading control. $N = 4$.

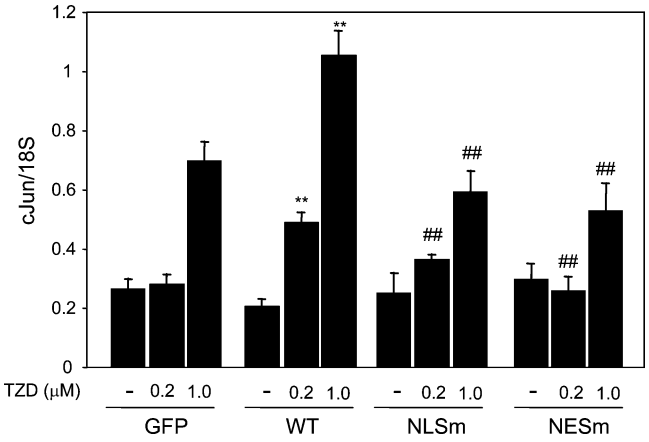

FIGURE 6: The NLS and the NES of FABP4 are required for enhancement of troglitazone-induced upregulation of cJun. MCF-7 cells were plated in 6-well plates in DMEM supplemented with 10% charcoal-treated FBS. Cells were transfected with expression vectors for GFP, or for GFP-tagged WT-FABP4, or denoted FABP4 mutants, grown overnight, and then treated with vehicle or with troglitazone in serum-free DMEM for 2 h. Expression of cJun mRNA was measured by Q-PCR. The results were analyzed with a 1-tailed Student's *t* test with pooled variances. (**) $P < 0.05$ compared to the GFP control. (##) $P < 0.05$ compared to WT-FABP4. $N = 3$.

the FABP4/PPARγ ligand troglitazone, enables ligand-activated nuclear import of the protein. Nuclear export of FABP4 is mediated by the CRM1 export machinery, and, in contrast with the ligand-inducible nuclear import, is not regulated by ligand. The nuclear export signal of FABP4 consists of three leucine residues, L66, L86, and L91. These residues are not adjacent in the primary sequence, but they form a leucine-rich motif, similar to established nuclear export signals, in the protein's tertiary structure. The observations that both the import and the export signals of FABP4 cannot be recognized in the primary sequence but are readily identifiable in the three-dimensional structure of the folded protein underscore the importance of detailed structural information for understanding structure/function relationships and for mapping critical motifs in proteins and protein families.

The requirements for nucleocytoplasmic shuttling of FABP4 for the cooperation of this protein with PPARγ were examined by utilizing a reporter gene construct, as well as by monitoring expression levels of the endogenous PPARγ target gene cJun. The data demonstrate that both the nuclear import and the active nuclear export of FABP4 are critical for enabling the protein to enhance the transcriptional activity of the receptor. Nuclear import, which is triggered by an activating ligand, allows FABP4 to shuttle specific ligands from the cytosol to PPARγ in the nucleus. The ligand-independent nuclear export ensures that FABP4 is not trapped in the nucleus, an outcome that will hamper the ability of the binding protein to access ligands that are generated in the cytosol.

It may be argued that the loss of the ability of the NLS and NES FABP4 mutants to enhance the activity of PPARγ may stem from disruption of the interactions of the binding protein with the receptor rather than from interference with the protein's nucleocytoplasmic trafficking. However, the observations that the mutations do not hamper high affinity binding of ligands by the protein attest to an intact three-dimensional fold. Also noteworthy in regard to this is that the nuclear receptor interaction domain of CRABP-II, a protein that shares with FABP4 a very similar three-dimensional structure, a homologous function, and an identical NLS, was previously mapped to residues G75, P81, and K102 (*57*). These residues are positioned far from both the NLS and the NES signatures. Specifically, the NLS and the receptor interaction domain are positioned on opposite sides of the entrance to the ligand binding pocket, while the NES residues lie at the bottom of the pocket (Figure 1a). In the 3-dimensional structure, these regions do not appear to be

```
FABP4 (a-fabp) 1 MCD--AFVGTWKLVSSENFDDYMKEVGVGFATRKVA--GMAKPNMIISVN
FABP5 (k-fabp) 1 MASLKDLEGKWRLMESHGFEEYMKELGVGLALRKMA--AMAKPDCIITCD
FABP7 (b-fabp) 1 MAD--AFVGTWKLVDSKNFDDYMKSLGVGFATRQVA--SMTKPTTIIEKN
FABP3 (h-fabp) 1 MVD--AFCATWKLTDSQNFDEYMKALGVGFATRQVG--NVTKPTVIISQE
FABP1 (l-fabp) 1 M----NFSGKYQLQSQENFEPFMK--AIGLPEDLIQKGKDIKGVSEIVHE
CRABP-II       1 MPN---FSGNWKIIRSENFEEMLKALGVNMMMRKIAVAAASKPAVEIKQE

FABP4 (a-fabp) 47 GDLVTIRSESTFKNTEISFKLGVEFDEITADDRKVKSIITLDGGALVQVQ
FABP5 (k-fabp) 49 GNNITVKTESTVKTTVFSCNLGEKFDETTADGRKTETVCTFQDGALVQHQ
FABP7 (b-fabp) 47 GDTITIKTQSTFKNTEINFQLGIEFDEVTADDRKVKSLVTLDGGKLIHVQ
FABP3 (h-fabp) 47 GGKVVIRTQCTFKNTEINFQLGEEFEETSIDDRNCKSVVRLDGDKLIHVQ
FABP1 (l-fabp) 45 GKKIKLTITYGPKVVRNEFTLGEECELETMTGEKVKAVVKLEGDNKMVTT
CRABP-II       48 NDTFYIKTSTTVRTTEINFKIGEEFEEQTVDGRPCKSLVKWESGNKMVCE
```

FIGURE 7: Alignment of iLBPs with regions of FABP4 containing the NLS and the NES. Some but not all iLBPs contain residues that correspond to the positively charged FABP4-NLS (bold) and the hydrophobic FABP4-NES (bold and underlined). Alignment was accomplished using accession numbers: mFABP4, NM_024406.1; mFABP5, NM_010634.1; mFABP3, NM_010174.1; mFABP7, NM_021272.2; mFABP1, NM_017399.1; mCRABP-II, NM_007759.1.

connected by any intramolecular bonds, suggesting that they function independently of one another.

Alignment of the primary sequences of several iLBPs (Figure 7) shows that the three leucine residues that comprise the NES of FABP4 are also present in FABP5, FABP7 (brain-FABP), and FABP3 (heart-FABP). Hence, these proteins may also possess a "3-dimensional NES" similar to that found in FABP4, and are likely to be involved in nuclear activities. Indeed, it has been reported that FABP5 functions to deliver ligands to PPARδ, and that FABP3 may cooperate with PPARα (*34*). The alignment also reveals that FABP1 (liver-FABP) does not possess either an NLS or an NES similar to those found in other FABPs, suggesting that it exerts its biological activities outside the nucleus or that it may get to the nucleus by a different type of a mechanism. It may be worth noting that, among iLBPs, FABP1 is unique in that its ligand-binding pocket can accommodate two fatty acids rather than the common 1:1 stoichiometry, and that it binds hydrophobic compounds larger than ligands that associate with other iLBPs (*55*). Hence, while it is becoming increasingly clear that some iLBPs closely cooperate with specific nuclear receptors and are activated by ligands that they share with their cognate receptors, the biological functions of FABP1 and the physiological ligands for this protein remain to be elucidated.

The data presented here and in a previous report (*33*) suggest that, despite the structural and functional similarities of FABP4 and CRABP-II, the former is actively exported from the nucleus, while the latter is not. In accordance with these conclusions, alignment of the primary sequences of the two proteins (Figure 7) shows that CRABP-II lacks the Leu residues that comprise the NES of FABP4, where their place is taken by Ile, Trp, and Lys. Notably, it was previously reported that endogenous CRABP-II in MCF-7 cells accumulates in the perinuclear region where it displays a punctate pattern, suggesting that it is associated with a specific subcellular organelle (*33*). It was also reported that apo-CRABP-II possesses biological activities that are unrelated to its ability to shuttle retinoic acid to RAR (*56*). Taken together, these observations suggest that the cytosolic localization of apo-CRABP-II is maintained by mechanisms other than active nuclear export. Such a mechanism could involve association with specific binding partners in the extranuclear milieu through which the protein may exert its retinoic acid-independent activities. Reversal of the association upon binding of retinoic acid allows CRABP-II to undergo nuclear localization and deliver the ligand to its cognate nuclear receptor, RAR.

Protein−ligand interactions have long been understood in terms of the "induced-fit" model which states that ligand-binding induces a protein to undergo conformational changes, and that such changes precede the formation of the activated holo-form (*37*). In contrast, the theory of "pre-existing equilibrium" postulates that apoproteins occupy multiple conformations where apo-like states are most probable, but others, which are conformationally compatible with ligand-binding, are present. When a ligand is introduced, ligand-compatible conformations are stabilized and become most probable (*38*). Several studies provided evidence for the role of pre-existing equilibria in protein interactions *in vitro* (*39*, *40*), but clear demonstration of the relevance of the model for the biological activities of proteins is lacking. We show here that, upon inhibition of its nuclear export, either by blocking the export machinery (Figure 1) or by mutating the protein's NES (Figure 2), a large fraction of FABP4 accumulates in the nucleus even in the absence of ligand. Hence, an import-competent conformation must exist in the apo-FABP4 population, enabling the protein to enter the nucleus in the absence of ligand. These observations thus provide strong support for the theory of pre-existing equilibrium and, to the best of our knowledge, comprise the first demonstration of the validity of the model in whole cells. The functional importance of stabilization of the import-competent form of the protein by the ligand becomes clearly evident in cells that actively export the protein, where ligand-binding is necessary for shifting the distribution toward the nucleus. The ligand-dependent nuclear import thus counteracts the constitutive export, enabling the continuous nucleocytoplasmic shuttling that is required for FABP4 function.

REFERENCES

1. Desvergne, B., and Wahli, W. (1999) *Endocr. Rev. 20*, 649−688.
2. Mueller, E., Sarraf, P., Tontonoz, P., Evans, R. M., Martin, K. J., Zhang, M., Fletcher, C., Singer, S., and Spiegelman, B. M. (1998) *Mol. Cell 1*, 465−470.
3. Koutnikova, H., Cock, T. A., Watanabe, M., Houten, S. M., Champy, M. F., Dierich, A., and Auwerx, J. (2003) *Proc. Natl. Acad. Sci. U.S.A. 100*, 14457−14462.
4. Alvarez, M., Rhodes, S. J., and Bidwell, J. P. (2003) *Gene 313*, 43−57.
5. Lazar, M. A. (2005) *Biochimie 87*, 9−13.
6. Zhang, L., and Chawla, A. (2004) *Trends Endocrinol. Metab. 15*, 500−505.
7. Castrillo, A., and Tontonoz, P. (2004) *Annu. Rev. Cell Dev. Biol. 20*, 455−480.
8. Theocharis, S., Margeli, A., Vielh, P., and Kouraklis, G. (2004) *Cancer Treat. Rev. 30*, 545−554.
9. Forman, B. M., Tontonoz, P., Chen, J., Brun, R. P., Spiegelman, B. M., and Evans, R. M. (1995) *Cell 83*, 803−812.
10. Staels, B. (2005) *Curr. Med. Res. Opin. 21* (Suppl. 1), S13−20.
11. Berger, J. P., Akiyama, T. E., and Meinke, P. T. (2005) *Trends Pharmacol. Sci. 26*, 244−251.
12. Fenner, M. H., and Elstner, E. (2005) *Expert Opin. Invest. Drugs 14*, 557−568.
13. Zang, C., Liu, H., Posch, M. G., Waechter, M., Facklam, M., Fenner, M. H., Ruthardt, M., Possinger, K., Phillip Koeffler, H., and Elstner, E. (2004) *Leuk. Res.* 28, 387−397.
14. Banaszak, L., Winter, N., Xu, Z., Bernlohr, D. A., Cowan, S., and Jones, T. A. (1994) *Adv. Protein Chem. 45*, 89−151.
15. Kleywegt, G. J., Bergfors, T., Senn, H., Le Motte, P., Gsell, B., Shudo, K., and Jones, T. A. (1994) *Structure* 2, 1241−1258.

16. Veerkamp, J. H., and Maatman, R. G. (1995) *Prog. Lipid Res. 34*, 17−52.
17. Kane, C. D., Lalonde, J. M., Banaszak, L. J., and Bernlohr, D. A. (1994) *J. Cell. Biochem.* 180−180.
18. Fiorella, P. D., and Napoli, J. L. (1991) *J. Biol. Chem. 266*, 16572−16579.
19. Bradbury, A., Possenti, R., Shooter, E. M., and Tirone, F. (1991) *Proc. Natl. Acad. Sci. U.S.A. 88*, 3353−3357.
20. Levin, M. S., Locke, B., Yang, N. C., Li, E., and Gordon, J. I. (1988) *J. Biol. Chem. 263*, 17715−17723.
21. Dong, D., Ruuska, S. E., Levinthal, D. J., and Noy, N. (1999) *J. Biol. Chem. 274*, 23695−23698.
22. Gutierrez-Gonzalez, L. H., Ludwig, C., Hohoff, C., Rademacher, M., Hanhoff, T., Ruterjans, H., Spener, F., and Lucke, C. (2002) *Biochem. J. 364*, 725−737.
23. Norris, A. W., and Spector, A. A. (2002) *J. Lipid Res. 43*, 646−653.
24. Widstrom, R. L., Norris, A. W., and Spector, A. A. (2001) *Biochemistry 40*, 1070−1076.
25. Hotamisligil, G. S., Johnson, R. S., Distel, R. J., Ellis, R., Papaioannou, V. E., and Spiegelman, B. M. (1996) *Science 274*, 1377−1379.
26. Makowski, L., Brittingham, K. C., Reynolds, J. M., Suttles, J., and Hotamisligil, G. S. (2005) *J. Biol. Chem. 280*, 12888−12895.
27. Makowski, L., and Hotamisligil, G. S. (2004) *J. Nutr. 134*, 2464S−2468S.
28. Maeda, K., Uysal, K. T., Makowski, L., Gorgun, C. Z., Atsumi, G., Parker, R. A., Bruning, J., Hertzel, A. V., Bernlohr, D. A., and Hotamisligil, G. S. (2003) *Diabetes 52*, 300−307.
29. Boord, J. B., Maeda, K., Makowski, L., Babaev, V. R., Fazio, S., Linton, M. F., and Hotamisligil, G. S. (2002) *Arterioscler. Thromb. Vasc. Biol. 22*, 1686−1691.
30. Makowski, L., Boord, J. B., Maeda, K., Babaev, V. R., Uysal, K. T., Morgan, M. A., Parker, R. A., Suttles, J., Fazio, S., Hotamisligil, G. S., and Linton, M. F. (2001) *Nat. Med. 7*, 699−705.
31. Celis, J. E., Ostergaard, M., Basse, B., Celis, A., Lauridsen, J. B., Ratz, G. P., Andersen, I., Hein, B., Wolf, H., Orntoft, T. F., and Rasmussen, H. H. (1996) *Cancer Res. 56*, 4782−4790.
32. Ohlsson, G., Moreira, J. M., Gromov, P., Sauter, G., and Celis, J. E. (2005) *Mol. Cell. Proteomics 4*, 570−581.
33. Sessler, R. J., and Noy, N. (2005) *Molecular Cell 18*, 343−353.
34. Tan, N. S., Shaw, N. S., Vinckenbosch, N., Liu, P., Yasmin, R., Desvergne, B., Wahli, W., and Noy, N. (2002) *Mol. Cell. Biol. 22*, 5114−5127.
35. Budhu, A. S., and Noy, N. (2002) *Mol. Cell. Biol. 22*, 2632−2641.
36. Manor, D., Shmidt, E. N., Budhu, A., Flesken-Nikitin, A., Zgola, M., Page, R., Nikitin, A. Y., and Noy, N. (2003) *Cancer Res. 63*, 4426−4433.
37. Koshland, D. E., Jr., Ray, W. J., Jr., and Erwin, M. J. (1958) *Fed. Proc. 17*, 1145−1150.
38. Gunasekaran, K., Ma, B., and Nussinov, R. (2004) *Proteins 57*, 433−443.
39. Foote, J., and Milstein, C. (1994) *Proc. Natl. Acad. Sci. U.S.A. 91*, 10370−10374.
40. Tobi, D., and Bahar, I. (2005) *Proc. Natl. Acad. Sci. U.S.A. 102*, 18908−18913.
41. Borst, D. E., Redmond, T. M., Elser, J. E., Gonda, M. A., Wiggert, B., Chader, G. J., and Nickerson, J. M. (1989) *J. Biol. Chem. 264*, 1115−1123.
42. Norris, A. W., Cheng, L., Giguere, V., Rosenberger, M., and Li, E. (1994) *Biochim. Biophys. Acta 1209*, 10−18.
43. Lin, Q., Ruuska, S. E., Shaw, N. S., Dong, D., and Noy, N. (1999) *Biochemistry 38*, 185−190.
44. Moroianu, J. (1999) *Crit. Rev. Eukaryotic Gene Expression 9*, 89−106.
45. Sweitzer, T. D., Love, D. C., and Hanover, J. A. (2000) *Curr. Top. Cell. Regul. 36*, 77−94.
46. Mattaj, I. W., and Englmeier, L. (1998) *Annu. Rev. Biochem. 67*, 265−306.
47. Xu, Z. H., Bernlohr, D. A., and Banaszak, L. J. (1993) *J. Biol. Chem. 268*, 7874−7884.
48. Shimada, T., Kojima, K., Yoshiura, K., Hiraishi, H., and Terano, A. (2002) *Gut 50*, 658−664.
49. Kilgore, M. W., Tate, P. L., Rai, S., Sengoku, E., and Price, T. M. (1997) *Mol. Cell. Endocrinol. 129*, 229−235.
50. Elstner, E., Muller, C., Koshizuka, K., Williamson, E. A., Park, D., Asou, H., Shintaku, P., Said, J. W., Heber, D., and Koeffler, H. P. (1998) *Proc. Natl. Acad. Sci. U.S.A. 95*, 8806−8811.
51. Wang, P., Palese, P., and O'Neill, R. E. (1997) *J. Virol. 71*, 1850−1856.
52. Wolff, T., Unterstab, G., Heins, G., Richt, J. A., and Kann, M. (2002) *J. Biol. Chem. 277*, 12151−12157.
53. Yamaki, A., Kudoh, J., Shimizu, N., and Shimizu, Y. (2004) *Biochem. Biophys. Res. Commun. 313*, 482−488.
54. Chkheidze, A. N., and Liebhaber, S. A. (2003) *Mol. Cell. Biol. 23*, 8405−8415.
55. Thompson, J., Ory, J., Reese-Wagoner, A., and Banaszak, L. (1999) *Mol. Cell. Biochem. 192*, 9−16.
56. Donato, L. J., and Noy, N. (2005) *Cancer Res. 65*, 8193−8199.
57. Budhu, A., Gillilan, R., and Noy, N. (2001) *J. Mol. Biol. 305*, 939−949.

BI700047A